

**Gaps and excitations in fullerides with partially filled bands: NMR study of Na<sub>2</sub>C<sub>60</sub> and K<sub>4</sub>C<sub>60</sub>**

V. Brouet and H. Alloul

*Laboratoire de Physique des Solides, UMR 8502 Université Paris-Sud, Bâtiment 510 91405 Orsay, France*

S. Garaj and L. Forró

*Laboratoire des solides semicristallins, IGA-Département de Physique, Ecole Polytechnique Fédérale de Lausanne, 1015 Lausanne, Switzerland*

(Received 28 February 2002; published 31 October 2002)

We present a nuclear magnetic resonance (NMR) study of Na<sub>2</sub>C<sub>60</sub> and K<sub>4</sub>C<sub>60</sub>, two compounds that are related by electron-hole symmetry in the C<sub>60</sub> triply degenerate conduction band. In both systems, it is known that NMR spin-lattice relaxation rate ( $1/T_1$ ) measurements detect a gap in the electronic structure, most likely related to singlet-triplet excitations of the Jahn-Teller distorted (JTD) C<sub>60</sub><sup>2-</sup> or C<sub>60</sub><sup>4-</sup>. However, the extended temperature range of the measurements presented here (10 K to 700 K) allows one to reveal deviations with respect to this general trend, both at high and low temperatures. Above room temperature,  $1/T_1$  deviates from the activated law that one would expect from the presence of the gap and saturates. In the same temperature range, a lowering of symmetry is detected by the appearance of quadrupole effects on the <sup>23</sup>Na spectra of Na<sub>2</sub>C<sub>60</sub>. In K<sub>4</sub>C<sub>60</sub>, modifications of the <sup>13</sup>C spectra line shapes also indicate a structural modification. We discuss this high-temperature deviation in terms of a coupling between JTD and local symmetry. At low temperatures,  $1/T_1T$  tends to a constant value for Na<sub>2</sub>C<sub>60</sub>, both for <sup>13</sup>C and <sup>23</sup>Na NMR. This indicates a residual metallic character, which emphasizes the proximity of metallic and insulating behaviors in alkali fullerides.

DOI: 10.1103/PhysRevB.66.155122

PACS number(s): 71.30.+h, 76.60.-k, 71.28.+d

**I. INTRODUCTION**

Soon after the discovery of fullerides, A<sub>4</sub>C<sub>60</sub> was found to behave as an insulator rather than the metal expected in a band picture.<sup>1</sup> The first indication for this was the detection by muon-spin resonance in K<sub>4</sub>C<sub>60</sub> of a muonium precession<sup>2</sup> at 5 K, which is known to be quickly suppressed in the presence of unpaired electrons. This signal disappears at higher temperatures suggesting the presence of thermally populated states. This has been confirmed by subsequent measurements of magnetic properties, electron-spin resonance (ESR) detects an activated susceptibility in K<sub>4</sub>C<sub>60</sub> with  $E_a = 60$  meV,<sup>3</sup> and superconducting quantum interference device (SQUID) measurements in Rb<sub>4</sub>C<sub>60</sub> yields  $E_a = 60$  meV.<sup>4</sup> An activated component has also been found in the nuclear magnetic resonance (NMR) relaxation rate  $1/T_1$  in K<sub>4</sub>C<sub>60</sub> with  $E_a = 55$  meV (Ref. 5) and Rb<sub>4</sub>C<sub>60</sub> with  $E_a = 70$  meV.<sup>6,7</sup> Other measurements also suggest an insulating ground state; no Fermi edge is visible by photoemission in K<sub>4</sub>C<sub>60</sub> and Rb<sub>4</sub>C<sub>60</sub> films<sup>8</sup> and no Drude peak is found by optical conductivity.<sup>9</sup> However, in this latter study, the gap to the lowest conductivity peak is significantly larger than in magnetic measurements, around 500 meV. A more recent investigation by electron-energy-loss spectroscopy (EELS) in transmission<sup>10</sup> also revealed a gap of the order of 500 meV in K<sub>4</sub>C<sub>60</sub> and Rb<sub>4</sub>C<sub>60</sub>. Therefore, two different gaps are necessary to describe these systems, a small “spin” gap of the order of 50–100 meV and a larger “optical” gap of about 500 meV. As no magnetism has ever been reported at low temperature, the ground state for C<sub>60</sub><sup>4-</sup> must be singlet and the small gap has been associated to singlet-triplet transitions.<sup>6,7,11</sup> The large gap is presumably a direct gap in

the substructure of the band. In addition, these systems are close to a metal-insulator transition, as shown by the transition to a metallic state observed by NMR at 12 kbars in Rb<sub>4</sub>C<sub>60</sub> (Ref. 7) and by the fact that the system with the smallest C<sub>60</sub>-C<sub>60</sub> distance, Na<sub>4</sub>C<sub>60</sub>, might even be metallic in its monomer phase ( $T > 500$  K), namely, a body-centered tetragonal (bct) structure,<sup>12,13</sup> isostructural to other A<sub>4</sub>C<sub>60</sub> systems.<sup>14</sup>

Understanding the origin of the insulating state is a necessary step to describe the physics of fullerides. Although the crystal field due to the bct structure is not sufficient to lift the threefold degeneracy of the  $t_{1u}$  band (the C<sub>60</sub> lowest unoccupied molecular orbital, filled with electrons brought by the alkali ions),<sup>1</sup> it has been suggested that this particular structure might explain why A<sub>4</sub>C<sub>60</sub> is insulating contrary to the metallic and face-centered-cubic (fcc) A<sub>3</sub>C<sub>60</sub> compounds.<sup>15</sup> Especially, the bct lattice is bipartite (contrary to the fcc one), which could play a role by enhancing antiferromagnetic correlations, hence favoring a Mott insulating state. However, we have shown recently that Na<sub>2</sub>C<sub>60</sub>, which is cubic,<sup>16</sup> exhibits a behavior similar to A<sub>4</sub>C<sub>60</sub>, with an activated temperature dependence of  $1/T_1$ .<sup>11</sup> Electron-hole symmetry then applies in the  $t_{1u}$  band and the detection of a gap is an intrinsic feature of fullerides with two or four electrons per ball rather than one of the bct structure.

There is a growing consensus that Jahn-Teller distortions (JTD) of the C<sub>60</sub> molecule are an essential ingredient for the insulating state of A<sub>4</sub>C<sub>60</sub>, although they have never been detected directly in these compounds.<sup>13</sup> Molecular calculations<sup>17</sup> indicate that the two most stable JTD correspond to the squeezing or elongation of the C<sub>60</sub> molecule around one of the three equivalent axes of the quasi spherical structure. This lifts the degeneracy of the  $t_{1u}$  levels by an amount of  $U_{JT} \approx 0.5$  eV, as sketched in Fig. 1. The most

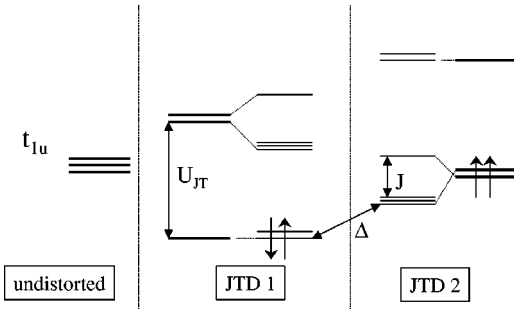


FIG. 1. Schematic representation of the structure of the three  $t_{1u}$  levels for two electrons per  $C_{60}$  and for the two most stable distortions (called JTD 1 and JTD 2) without spin degeneracy (thick lines) and with spin degeneracy (thin lines). The various gaps are indicated by arrows, the Jahn-Teller splitting  $U_{JT}$ , the exchange splitting  $J$ , and the singlet-triplet gap  $\Delta$  (adapted from Ref. 17).

stable JTD corresponds to a singlet ground state for  $C_{60}^{2-}$  (see the case JTD 1 in Fig. 1) and  $C_{60}^{4-}$  (case JTD 2), as observed experimentally. The first excited state of a  $C_{60}^{2-}$  is a triplet corresponding to JTD 2. It lies about  $\Delta = 100$  meV higher in energy, which is consistent with the experimentally measured spin gap.

In the solid, two different situations could occur, either a cooperative JTD or independent (and possibly dynamic) JTD for each molecule. In the first case, a band gap would open if the cooperative distortion is commensurate with the lattice. The second scenario is considered to be the most likely for fullerides due to the unusually large quantum fluctuations in the  $C_{60}$  molecule.<sup>18,19</sup> Another kind of excitation could take place between the  $t_{1u}$  levels split by the JTD, and  $U_{JT} = 500$  meV would correspond to the large “direct” optical gap. Let us emphasize that, as  $U_{JT}$  has the same order of magnitude as the bandwidth  $W$ , the gap in other directions could be much smaller. This is why Fabrizio and Tosatti have proposed that strong electronic correlations are necessary in addition to JTD to understand the insulating state, which could be called a Mott-Jahn-Teller ground state.<sup>18</sup> As we have seen, this model is supported by the large body of experiments in  $Na_2C_{60}$  and  $A_4C_{60}$ , because it explains the occurrence of two gaps and predicts the correct order of magnitude for them.

In this paper, we will first introduce the basic NMR facts indicating that  $Na_2C_{60}$  and  $K_4C_{60}$  are insulators with similar properties and are in good agreement with the Mott-JT model described previously (Sec. II). We then present data up to very high temperatures (700 K) that call for a more refined model than a simple thermal population of an excited state. We suggest in Sec. III that subtle changes in local symmetry detected by NMR near room temperature could be a relevant parameter to explain the high-temperature evolution of the physical properties. The structural modifications likely couple to the JTD and might modify the equilibrium between singlet and triplet states. In Sec. IV, we will study in detail the question of a possible coexistence of metallic behavior in  $Na_2C_{60}$  with the aforementioned molecular excitations. As explained previously, this is not inconsistent with the Mott-JT scenario. The status of JTD in a metallic or

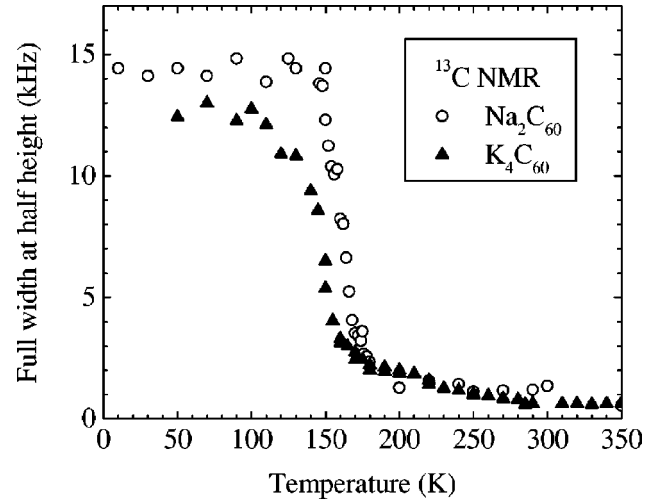


FIG. 2.  $^{13}C$  NMR linewidth as a function of temperature for  $Na_2C_{60}$  and  $K_4C_{60}$ . The broadening of the spectra due to the slowing down of the  $C_{60}$  molecular motions is visible around 150 K.

semimetallic environment is actually an important issue to clarify. This paper is the first of a series of three papers [called hereafter I, II,<sup>20</sup> and III (Ref. 21)] focused on this problem.

## II. A NONMAGNETIC GROUND STATE WITH GAPPED EXCITATIONS

In this section, we show that the  $^{13}C$  NMR spectra shifts, and line shapes, as well as the dynamic susceptibility monitored by the spin-lattice relaxation rate  $1/T_1$ , exhibit similar features in  $Na_2C_{60}$  and  $K_4C_{60}$ . Both compounds are characterized by a nonmagnetic ground state and a gap in their low-energy excitations. We present measurements above room temperature that allow to investigate this behavior in greater detail.

### A. $^{13}C$ NMR spectra

Let us detail first that the evolution of the  $^{13}C$  NMR spectra at low temperatures, shown in Fig. 2, clearly demonstrates that no magnetic transition occurs in  $Na_2C_{60}$  and  $K_4C_{60}$ . To understand this, let us first recall the interactions contributing to the shift  $K$  of one NMR line,

$$\bar{K} = \bar{\sigma} + \bar{A} \bar{\chi}. \quad (1)$$

$\bar{\sigma}$  represents a chemical shift tensor and  $\bar{A} \bar{\chi}$  the contribution from unpaired electrons called the Knight shift.  $\bar{A}$  is the hyperfine coupling tensor between  $^{13}C$  and unpaired electrons and  $\chi$  the local electronic susceptibility. All these quantities have both isotropic and anisotropic parts. In the case of  $C_{60}$  compounds, the anisotropic part is usually the largest, because electrons reside mainly in orbitals with a pronounced  $p$  character. As these orbitals have nodes at the nuclear position, the electrons do not interact directly with the  $^{13}C$  nuclear spin through the so-called contact interaction, and the hyperfine coupling is mainly of dipolar origin.<sup>22</sup> As a consequence, the shift is a function of the orientation of one orbital with respect to the NMR applied field. At high temperatures, when the molecules are rapidly rotating, the aniso-

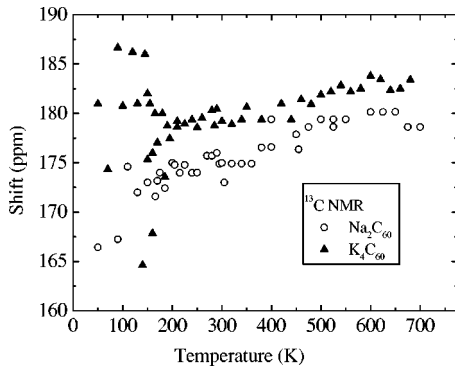


FIG. 3. Temperature dependence of the shift (with respect to TMS) of the center of gravity of the  $^{13}\text{C}$  NMR spectra in  $\text{Na}_2\text{C}_{60}$  and  $\text{K}_4\text{C}_{60}$ . The accuracy is lower at low temperatures because of the broadening of the spectra.

tropic contribution is averaged out and narrow lines are observed. They broaden when the motions slow down and appear static on the NMR time scale (a few milliseconds). This has been observed in many fullerides and Fig. 2 shows that this takes place at 150 K in the case of  $\text{K}_4\text{C}_{60}$  and 160 K for  $\text{Na}_2\text{C}_{60}$ . We note that the time scale of the  $\text{C}_{60}$  motion appears to be similar in both compounds, despite the different structures and presumably different interactions between  $\text{C}_{60}$  and K or Na.

There is no further broadening of the spectra below this temperature, which means that there is *no magnetic transition* at least down to the lowest measured temperature, 10 K in  $\text{Na}_2\text{C}_{60}$  and 50 K in  $\text{K}_4\text{C}_{60}$ . Indeed, static magnetic moments would create a large local magnetic field on  $^{13}\text{C}$  nuclei and cause a large broadening of the spectra in these powder samples. This finding is a key element for involving Jahn-Teller distortions in the description of these materials, because they explain naturally the singlet ground state. Otherwise, one could have rather expected a magnetic ground state for localized electrons, because Hund's rule should favor a high-spin state in the  $t_{1u}$  levels.

Relevant information about the insulating state should be found in the temperature dependence of the static spin susceptibility, which could, in principle, be extracted from the isotropic part of the Knight shift. Figure 3 shows that this is difficult because the isotropic shift (defined as the center of gravity of one spectrum) is small with respect to the line-width, especially at low temperature. In pure  $\text{C}_{60}$ , an isotropic chemical shift  $\sigma = 143$  ppm is observed,<sup>23</sup> characteristic of the orbital currents flowing in the filled orbitals. This is expected to be of the order of magnitude of the reference for the Knight shift in alkali fullerides. This idea was confirmed by the close value of 156 ppm found in the band insulator  $\text{A}_6\text{C}_{60}$ ,<sup>24</sup> which suggests an empirical correlation for  $\sigma$  of +1.5 ppm per added electron.<sup>25</sup> In  $\text{K}_4\text{C}_{60}$  and  $\text{Na}_2\text{C}_{60}$ , the shifts are, however, much larger than what would be expected with such a contribution for  $\sigma$  alone. At room temperature  $K = 175$  ppm for  $\text{Na}_2\text{C}_{60}$  and 179 ppm in  $\text{K}_4\text{C}_{60}$ , which is comparable to shifts measured in metallic  $\text{A}_3\text{C}_{60}$  (189 ppm in  $\text{K}_3\text{C}_{60}$ , for example<sup>26</sup>). This sizable Knight shift indicates the presence of electronic excitations giving rise to a large electronic susceptibility at room temperature.

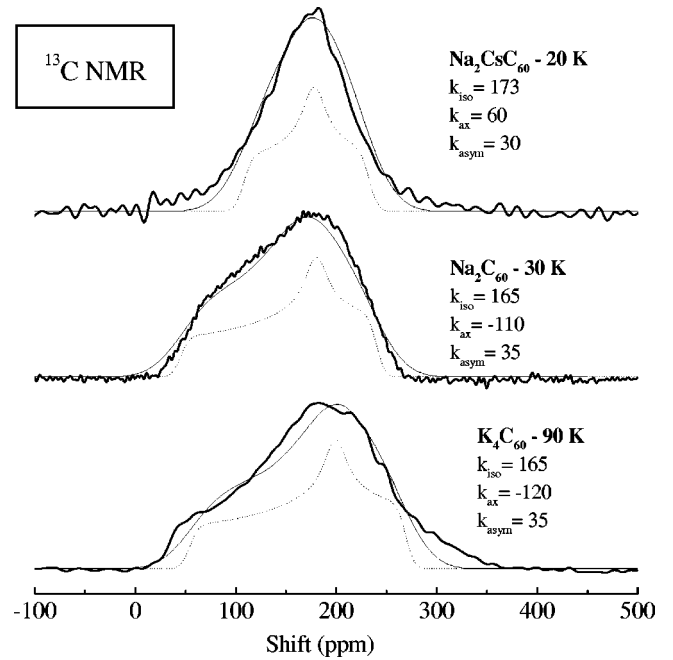


FIG. 4.  $^{13}\text{C}$  NMR spectra at low temperatures for  $\text{K}_4\text{C}_{60}$ ,  $\text{Na}_2\text{C}_{60}$ , and  $\text{Na}_2\text{CsC}_{60}$  (thick lines). Fit to a powder pattern of the anisotropic NMR shift [Eq. (2)] are also presented with parameters indicated on the figure. The thin solid line is obtained by a convolution of the theoretical line shape with a Gaussian of half-width at half maximum 35 ppm. A convolution with a 10-ppm-large Gaussian is also shown (dotted line) that reveals more clearly the underlying structure of the spectra.

At low temperature, the anisotropic part of the shift, which is also proportional to the susceptibility, can be studied as well. Typical  $^{13}\text{C}$  line shapes are presented in Fig. 4, they are similar in  $\text{Na}_2\text{C}_{60}$  and  $\text{K}_4\text{C}_{60}$  with a shoulder on the low-frequency side, characteristic of the chemical shift anisotropy found in pure  $\text{C}_{60}$ .<sup>23</sup> This can be stated more quantitatively if one extracts the parameters for the shift tensor by fitting the spectra to the theoretical powder pattern.<sup>27</sup> Defining

$$K = K_{iso} + K_{ax} \left( \frac{3 \cos^2 \theta - 1}{2} \right) + K_{asym} \sin^2 \theta \cos 2\varphi, \quad (2)$$

where  $\theta$  and  $\varphi$  are the spherical coordinates for the orientation of the principal axis of the tensor with respect to the applied magnetic field, one can compute the actual line shape by averaging on all possible orientations. The values found for  $\text{Na}_2\text{C}_{60}$  and  $\text{K}_4\text{C}_{60}$  are reported in Fig. 4, together with the fit of the experimental spectra. A convolution with a Gaussian function of width 35 ppm has been used to take into account an experimental broadening and reproduce the spectra. Because the parameters are not independent, we estimate an error of  $\pm 5$  ppm for each of them.  $K_{ax}$  and  $K_{asym}$  are very similar to the parameters found in pure  $\text{C}_{60}$  [ $K_{ax} = -110$  ppm and  $K_{asym} = 35$  ppm (Ref. 23)] even though the spectra are shifted by about 20 ppm. In contrast, it has been observed that for metallic  $\text{A}_3\text{C}_{60}$  compounds, the addition of the Knight shift anisotropy leads to *narrower* and

more *symmetric* lines. This is illustrated by the spectra in  $\text{Na}_2\text{CsC}_{60}$  also shown in the figure. Therefore, the observation of the typical  $\text{C}_{60}$  line shape in  $\text{Na}_2\text{C}_{60}$  and  $\text{K}_4\text{C}_{60}$  is a sign that the contribution of conduction electrons is weak at low temperature. The relatively large value found for the isotropic coupling ( $K = 165$  ppm) might be due to a slightly larger value of  $\sigma$  than that estimated previously.

The susceptibility then increases from a small value at low temperature to a sizable one at room temperature, which is consistent with the presence of singlet-triplet excitations proposed in the Introduction. We will see in the course of this paper that we can confirm the presence of these excitations more accurately using other NMR probes.

## B. $^{13}\text{C}$ NMR spin-lattice relaxation

### 1. Detection of a gap in the electronic structure

The most efficient way to detect these excitations is through spin-lattice relaxation measurements ( $1/T_1$ ), which measure the imaginary part of the electronic susceptibility, that is, if no particular  $q$  dependence is expected,

$$\frac{1}{T_1} = \frac{k_B T}{\hbar} A^2 \frac{\chi''(\omega_0)}{\omega_0}. \quad (3)$$

As can be seen in Fig. 5,  $1/T_1$  increases steeply with temperature for both compounds; the increase starts around 150 K in  $\text{K}_4\text{C}_{60}$  and 200 K in  $\text{Na}_2\text{C}_{60}$ . This has been observed previously (see Ref. 5 for  $\text{K}_4\text{C}_{60}$  and Ref. 11 for  $\text{Na}_2\text{C}_{60}$ ) and can be attributed to a gap related to singlet-triplet transitions between two different JTD's, as explained in the Introduction. The lines in Fig. 5 correspond to activated laws with  $E_g = 70$  meV for  $\text{K}_4\text{C}_{60}$  and  $E_g = 140$  meV for  $\text{Na}_2\text{C}_{60}$  and they describe the data correctly up to room temperature. At higher temperature, deviations are observed, which will be discussed in the last paragraph of this section. In  $\text{Rb}_4\text{C}_{60}$ , the activated part of  $1/T_1$  below 250 K is almost quantitatively identical to that of  $\text{K}_4\text{C}_{60}$ .<sup>7</sup> This could mean that the 70 meV gap is characteristic of a JT  $\text{C}_{60}^{4-}$ , while it is nearly twice as large for  $\text{C}_{60}^{2-}$ . However, we will argue in this paper that the gap extracted from  $1/T_1$  could be slightly different from the molecular value, because it is sensitive to the details of the local structure. Besides stoichiometry, one similarity between  $\text{K}_4\text{C}_{60}$  and  $\text{Rb}_4\text{C}_{60}$  that contrasts with  $\text{Na}_2\text{C}_{60}$  is precisely that they both have a bct structure and this could also explain the different gap values.

In a previous study,<sup>5</sup> Zimmer *et al.* have proposed a smaller gap in  $\text{K}_4\text{C}_{60}$  (50 meV), because they assign part of the increase of  $1/T_1$  to a molecular motion peak. They suggested that  $1/T_1$  would follow the dashed line of Fig. 5, once this peak is subtracted. By extending the measurement to higher temperature, we show that  $1/T_1$  on the contrary *saturates* above 250 K towards  $1/T_1 = \text{cst}$ , which invalidates this analysis. As for a molecular motion peak, Fig. 5 shows that it is unambiguously resolved at 180 K for  $\text{Na}_2\text{C}_{60}$ , but it does not appear clearly for  $\text{K}_4\text{C}_{60}$ . In the following section, we study this contribution in greater detail, to determine to what extent it could modify the shape of  $1/T_1$  vs  $T$ .

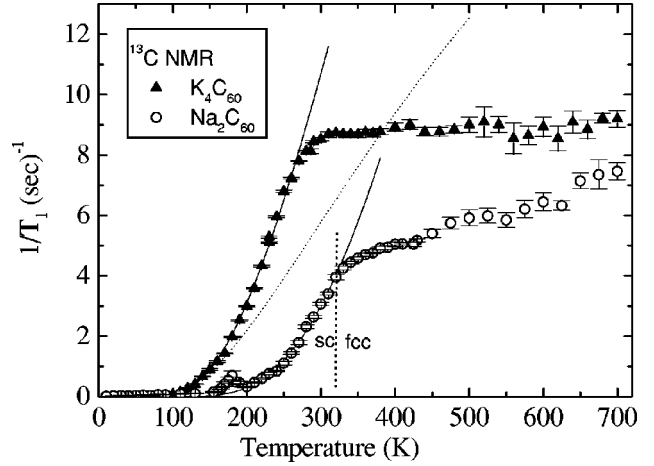


FIG. 5.  $^{13}\text{C}$  NMR  $1/T_1$  in  $\text{Na}_2\text{C}_{60}$  and  $\text{K}_4\text{C}_{60}$  from 10 to 700 K. Solid lines are fitted to an activated law below room temperature. The dashed line for  $\text{K}_4\text{C}_{60}$  is an extrapolation of the electronic contribution to  $1/T_1$  given in Ref. 5 based on data below 300 K and assuming a contribution from molecular motion peak.

### 2. Realistic parameters for the molecular motion peak contribution

Indeed, molecular motions have been found to contribute to  $1/T_1$  in different fullerides, most notably pure  $\text{C}_{60}$  (Ref. 23) and  $\text{K}_3\text{C}_{60}$ .<sup>28</sup> This is due to the fact that the local magnetic field  $H_{loc}$  sensed by  $^{13}\text{C}$  nuclear spin depends on the orientation of the  $p_z$  orbital, nearly perpendicular to the  $\text{C}_{60}$  ball at one carbon site, with respect to the NMR applied field. Rotation of the ball will *modulate* this local field. If the time scale of the motions is such that they create fluctuations of  $H_{loc}$  at the nuclear Larmor frequency  $\omega_0$ , they can relax the NMR nuclei. For fullerides, the fast rotation of the  $\text{C}_{60}$  molecule around one axis can be described by a frequency  $1/\tau$  that is typically of the order of  $\omega_0$  for temperatures around 200 K–400 K. A Bloembergen-Purcell-Pound peak<sup>29</sup> can be expected in this temperature range with

$$\frac{1}{T_1} = \alpha (\gamma H_{loc})^2 \frac{2\tau}{1 + (\omega_0\tau)^2}, \quad (4)$$

where  $\gamma$  is the gyromagnetic ratio for the nuclei and  $\alpha$  is a numeric prefactor of order unity, which depends on the details of the molecular motion.

To determine the actual value of  $\alpha$ , the anisotropy of  $H_{loc}$ , measured from the low-temperature spectra, should be used and the molecular motion should be modeled in an appropriate way, for example, a uniaxial rotation along one diagonal axis, following Ref. 30. The maximum value of  $\alpha$  is 1 if the local field is assumed to fluctuate randomly between two values<sup>27</sup>  $\pm H_{loc}$  but it can be much smaller, for example 6/40 in the case of random molecular reorientation for an axial symmetry of the shift tensor.<sup>31</sup> Here, we want to estimate  $\alpha$  from the experiment rather than from a theoretical model; to do so, some typical molecular contributions to  $1/T_1$  are shown in Fig. 6.

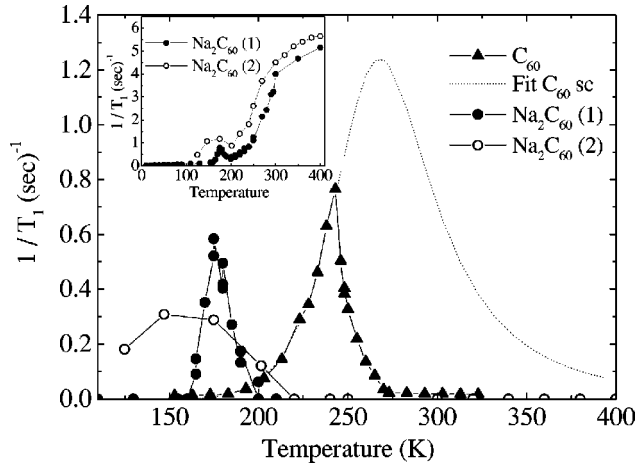


FIG. 6. Comparison of the molecular motion peak contribution to  $1/T_1$  in pure  $C_{60}$  (Ref. 23) and two  $Na_2C_{60}$  samples. The dashed line is a fit of the molecular motion in the sc phase of  $C_{60}$  ( $T < 260$  K) given in Ref. 23. Inset:  $1/T_1$  as a function of temperature in the two  $Na_2C_{60}$  samples.

From Eq. (4), it can be seen that the maximum of  $1/T_1$  occurs for  $\omega_0\tau=1$  with a value *depending uniquely on the linewidth*  $\Delta\nu=\gamma H_{loc}/2\pi$ . It is given by  $(1/T_1)_{max}=\alpha(\gamma H_{loc})^2/\omega_0$ . We have shown in the preceding section that  $K_4C_{60}$ ,  $Na_2C_{60}$ , and  $C_{60}$  exhibit roughly the same linewidth, so that similar contributions should be expected. Pure  $C_{60}$  is the simplest case because the relaxation is dominated by molecular motions, and the field dependence predicted by Eq. (4) has been successfully checked.<sup>32</sup> The data from Ref. 23 are reported in Fig. 6, and yield  $(1/T_1)_{max}=0.8\text{ sec}^{-1}$ . Let us note that these authors have extrapolated a “true” maximum  $(1/T_1)_{max}=1.2\text{ sec}^{-1}$  (dashed line), assuming that the peak is “cut” by the orientational transition at 260 K. This order of magnitude is consistent with the peak  $(1/T_1)_{max}=0.6\text{ sec}^{-1}$  found in  $Na_2C_{60}$ . When looking at Fig. 5, it is clear that a contribution of the order of  $1\text{ sec}^{-1}$  would not severely affect our discussion of  $K_4C_{60}$ .

The width of the peak depends on the variation of  $\tau$  with temperature and an Arrhenius law  $\tau=\tau_0\exp(E_a/T)$  is usually used, where  $E_a$  is the activation energy for the molecular motion and  $1/\tau_0$  the attempt frequency. These parameters are probably similar for different compounds and a typical width of about 50 K can be deduced from Fig. 6. Interestingly, we have found a significant difference between two  $Na_2C_{60}$  samples, called (1) and (2) in Fig. 6. The results presented here are from sample (1), sample (2) exhibits a similar behavior but seems to be of somewhat poorer quality, as can be seen by the slightly shorter  $T_1$  values (see inset of Fig. 6) or slightly broader linewidth. The molecular motion peak, although clearly present, is broader in sample (2), which is likely due to a distribution of the motion parameters, and consequently its maximum amplitude is smaller. Data in Fig. 5 imply that, if present, the peak in  $K_4C_{60}$  must be very broad, which could be due to sample quality or intrinsic disorder of the bct phase. Its intensity would be accordingly reduced, so that its contribution is furthermore negligible.

### 3. High-temperature behavior

The  $1/T_1=cst$  law observed at high temperatures in  $K_4C_{60}$  is then intrinsic. It is somewhat unusual as most relaxation mechanisms give an increasing relaxation rate with increasing temperature. Such a flat behavior is reminiscent of the relaxation observed in dense paramagnets, which is caused by a coupling to localized paramagnetic centers. Within our model of singlet-triplet (ST) excitations of JTD balls, we do have such centers at high temperatures, namely the triplet states. Nevertheless, our first expectation would be to observe such a law only when the population of these levels saturates, for temperatures above the ST gap, i.e.,  $T > 800$  K. More correctly, as  $1/T_1$  measures the imaginary part of the electronic susceptibility [see Eq. (3)], it is sensitive to both the *nature* and the *dynamics* of the relevant electronic excitations. In our case, this means that both the number and the lifetime of the triplet states contribute to  $1/T_1$ , so that an abrupt change in the temperature dependence of one of these quantities could explain the change in  $1/T_1$ . In  $Na_2C_{60}$ , we observe a similar deviation from the activated law before the expected saturation for  $k_B T = E_g$ , although it is not constant like in  $K_4C_{60}$ , but keeps increasing slightly up to 700 K. As the deviation is present in both systems, it must contain some insights of their physics.

The first possibility is that the activated law fails to describe the data over the full temperature range because there are other thermally accessible excitations, for example the singlet state of JTD 2 in Fig. 1, if  $J$  is small enough. A variant of this idea is that the arrangement of the molecular levels could be modified with increasing temperature. JTD being sensitively coupled to the crystal field of the structure, it is likely that even small structural modifications could affect the equilibrium between different JTD. A second possibility that goes beyond this “molecular approach,” is related to the fact that we deal here with solids that are very close to a metal-insulator transition, where hopping is certainly not strictly forbidden. The introduction of a hopping term in the JT Hamiltonian mixes different molecular states and can also affect the nature of the ground state. An estimation of the temperature dependence of the lifetime of the triplet state is obviously a complicated problem, as it probably involves both the dynamics of the Jahn-Teller distortion and hopping rates as a function of temperature. As an example, if a static distortion, for example due to a cooperative effect is stabilized at low temperatures, it could certainly affect  $1/T_1$ .

In any case, the evolution of  $1/T_1$  at high temperature cannot be understood with a model of isolated molecules, and forces us to take into account interactions between the balls and/or with the structure. For  $Na_2C_{60}$ , it is, for example, suggestive that  $1/T_1$  departs from the activated behavior near the temperature of the structural orientational transition taking place at 310 K.<sup>16</sup> In an attempt to identify the origin of the change in  $1/T_1$ , we now turn our attention to details of the structure that can be studied by NMR to see whether there is any detectable change in the corresponding temperature range.

### III. INTERPLAY BETWEEN JTD AND LOCAL SYMMETRY

There are very few cases where Jahn-Teller distortions have been observed directly in fullerides. One example is

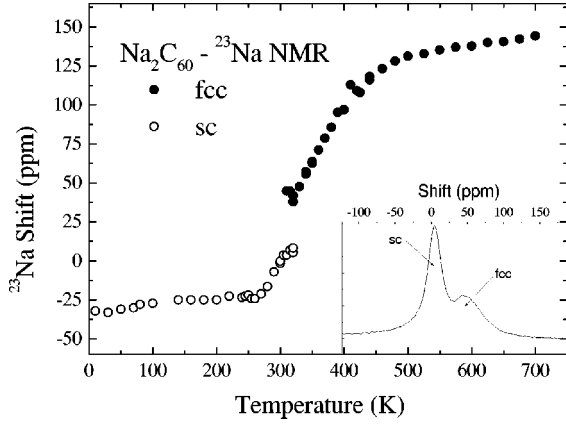


FIG. 7.  $^{23}\text{Na}$  NMR shifts (with respect to NaCl) in  $\text{Na}_2\text{C}_{60}$  for the fcc phase (solid circles,  $T > 310$  K) and the sc phase (open circles). Inset:  $^{23}\text{Na}$  spectrum at 310 K showing the coexistence of the two structures.

$\text{C}_{60}$ -tetraphenylphosphonium bromide, a salt where  $\text{C}_{60}^-$  molecules are well separated from each other. A cooperative Jahn-Teller state is thought to develop below 120 K, because a splitting of the Lande factor has been observed by ESR below 120 K.<sup>33</sup> Interestingly, a transition to an orientationally ordered state is observed at about the same temperature,<sup>34</sup> so that it seems likely that the new orientational order stabilizes the collective distortion. This example motivates us to relate to structural modifications the particular evolution of  $1/T_1$  at high temperatures. NMR, and especially alkali NMR, has proved to be a very sensitive probe for small structural distortions in fullerides.<sup>22</sup> We first focus on the effect of the structural transition in  $\text{Na}_2\text{C}_{60}$  on the electronic properties, as seen by  $^{23}\text{Na}$  NMR. We then review other signs of structural evolution in  $\text{Na}_2\text{C}_{60}$  and  $\text{K}_4\text{C}_{60}$  that indeed seem to coincide with the change in the electronic behavior.

#### A. Structural transition in $\text{Na}_2\text{C}_{60}$ studied by $^{23}\text{Na}$ NMR

Although the orientational transition taking place at 310 K could appear first as a minor structural change, it has often been argued in the case of  $n=3$  that sc phases behave quite differently from fcc phases.<sup>35</sup> For  $\text{Na}_2\text{C}_{60}$ , it seems reasonable to assume that at least some parameters (such as the gap value) could be different on both sides of the transition. Fitting the temperature dependence of  $\chi$  or  $1/T_1$  then becomes more difficult. This can be clarified by  $^{23}\text{Na}$  NMR because  $^{23}\text{Na}$  spectra differ in the two phases, which allows to discriminate what happens in the sc and fcc phases, respectively. In the inset of Fig. 7, a spectrum at 310 K shows the coexistence of the two phases, which we observe from 300 K to 315 K. Following the shift of each line, as done in Fig. 7, we can extract the susceptibility in both phases independently and observe that  $\chi$  increases in *both* sc and fcc phases. We also clearly see that a “saturation” appears in the fcc phase at 400 K, and not at the structural transition. This contradicts the impression given by  $^{13}\text{C}$   $1/T_1$ , which seems to change at the structural transition, but this is more reliable as  $^{13}\text{C}$  NMR does not resolve the signals of the two phases.

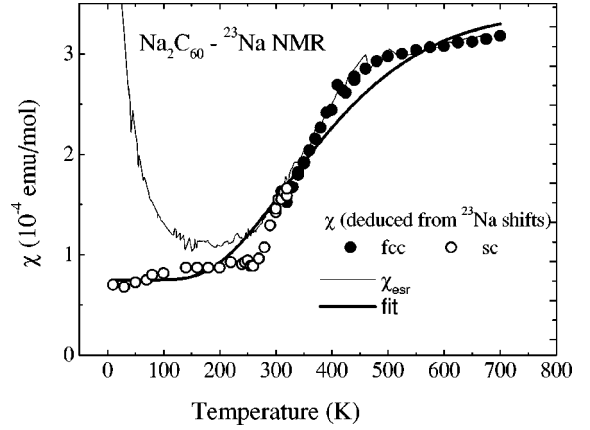


FIG. 8. ESR susceptibility measured on the same  $\text{Na}_2\text{C}_{60}$  batch as the NMR sample (thin line). Symbols represent an extrapolation of the true susceptibility extracted from  $^{23}\text{Na}$  NMR shifts as explained in the text. The thick line is a fit to the model described in the text [Eq. (5)].

In the fcc phase, the scaling between  $K$  and the ESR susceptibility is excellent (see Fig. 8) and the hyperfine coupling  $A_{fcc}$  can be extracted using Eq. (1), provided that  $\sigma_{fcc}$  is temperature independent (which is a usual assumption). We obtain  $\sigma_{fcc} = -65$  ppm and  $A_{fcc} = 3500$  Oe/ $\mu_B$ . The evolution of the susceptibility in the sc phase is especially interesting as the ESR susceptibility is masked by a large Curie term below 200 K. Following Eq. (1), the discontinuity at the transition could be attributed either to a different hyperfine coupling  $A$  or to a different susceptibility. The hyperfine coupling is defined by the local environment of a Na atom, which is indeed very different in sc or fcc phases. In the fcc phase, the orientations of the four neighboring  $\text{C}_{60}$  balls are such that Na faces four hexagonal rings, whereas, in the sc phase, it faces only one hexagonal ring and three double bonds (see Ref. 36 and Fig. 9). Therefore, there are probably two different hyperfine couplings  $A_{sc}$  and  $A_{fcc}$ . As ESR or  $^{13}\text{C}$   $1/T_1$  do not exhibit any obvious discontinuity at the transition,  $\chi$  is more likely to be continuous. Assuming that  $\sigma$  and  $\chi$  do not change at the transition, we find  $A_{sc} = 2300$  Oe/ $\mu_B$  and the variation of  $\chi$  deduced from NMR is reported in Fig. 8 by open circles for the sc phase.

We can now compare this refined estimation of  $\chi$  to the singlet-triplet model. A first conclusion is that  $\chi$  tends to a constant value at low temperatures corresponding to  $\chi = 7 \times 10^{-5}$  emu/mol. Although, this is somehow dependent on our assumption that  $\sigma_{sc} = \sigma_{fcc}$ , we have found a very similar value ( $6 \times 10^{-5}$  emu/mol) when trying to compare directly  $T_1$  and  $\chi_{esr}$  in Ref. 11, which gives some confidence in this estimate. This suggests the presence of a Pauli-like contribution in  $\text{Na}_2\text{C}_{60}$ , the likelihood of which will be discussed in the Sec. IV of this paper.

For the activated part, the singlet-triplet model of Fig. 1 predicts a susceptibility  $\chi(T) = n(T)\chi(S_1)$ , where  $n(T)$  is the number of thermally populated triplet states and  $\chi(S_1)$  is the Curie susceptibility for triplet states:

$$\chi(T) = \frac{3 \exp(-\Delta/T)}{2 + 3 \exp(-\Delta/T)} \frac{8\mu_B^2}{3k_B T} \quad (5)$$

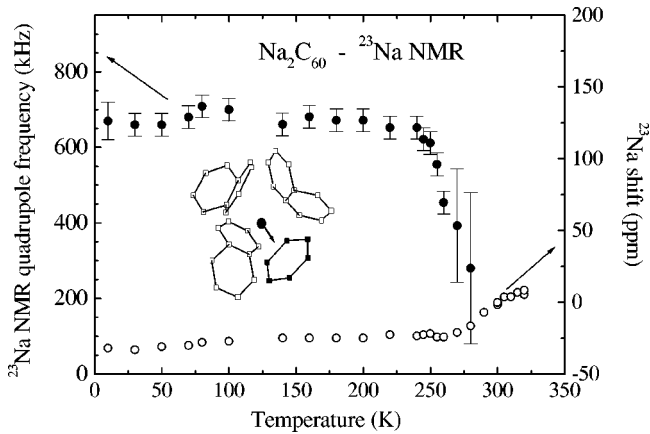


FIG. 9. Structural distortion in  $\text{Na}_2\text{C}_{60}$  evidenced by the appearance of a nuclear quadrupole frequency in the  $^{23}\text{Na}$  spectra below 250 K (solid points, right scale). It suggests that the distortion is due to a displacement of Na towards the hexagon of one of its four  $\text{C}_{60}$  neighbors. Left scale:  $^{23}\text{Na}$  NMR shift that starts increasing when the quadrupole frequency disappears.

The thick line in Fig. 7 is a fit to such a relation with  $\Delta = 100$  meV, which is 25% smaller than by using the estimation based on  $1/T_1$  data below room temperature. Quantitatively, the measured susceptibility corresponds to 80% of that estimated by Eq. (5), which sounds reasonable. Although this law clearly captures much of the physics of this phase, it does not fit our data satisfactorily over the whole  $T$  range. We observe a steeper increase of the susceptibility at 250 K and a larger inflection at 450 K. This suggests that *something else* might come into play at these temperatures, which helps or hinders the population of triplet states, and which it is not purely a thermal process. One of the possibilities that comes into mind is a small structural modification that would stabilize a particular state.

### B. Quadrupole effects on $^{23}\text{Na}$ in $\text{Na}_2\text{C}_{60}$

If the orientational structural transition does not seem to modify deeply the behavior of  $\text{Na}_2\text{C}_{60}$ , we present here the observation of further changes in local symmetry occurring in the sc phase that could couple to Jahn-Teller distortions and interact with the electronic properties.

As  $^{23}\text{Na}$  is a spin 3/2, it is sensitive to electric-field gradients (EFG) arising from deviations from cubic symmetry at the Na site. In the fcc phase, there are no detectable quadrupole effects, as expected in the cubic environment of one tetrahedral site. However, in the sc phase, a decrease in the NMR intensity at the fcc to sc transition indicates that quadrupole effects are present. In this case, the  $(-3/2 \rightarrow -1/2)$  and  $(1/2 \rightarrow 3/2)$  nuclear transitions are wiped out of the spectrum and only the central nuclear transition  $(1/2 \rightarrow -1/2)$  is detected. Below 200 K, a splitting of this central transition, which is characteristic of second-order broadening by the EFG is detected.<sup>31</sup> The  $(1/2 \rightarrow -1/2)$  line can be fitted at 100 K by an EFG tensor with a quadrupole frequency  $\nu_q = 700$  kHz and a small asymmetry  $\eta = 0.2$ .<sup>37</sup> The evolution of  $\nu_q$  with temperature is displayed in Fig. 9, it shows

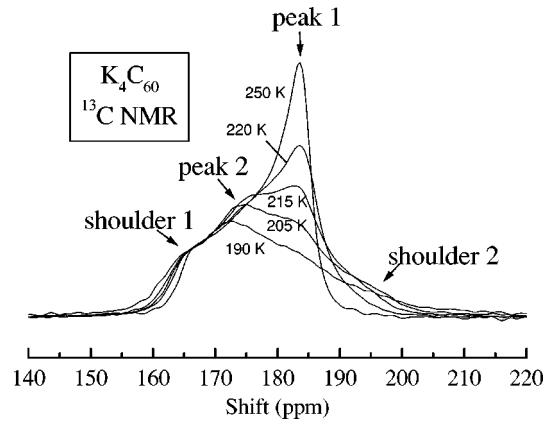


FIG. 10.  $^{13}\text{C}$  NMR spectra in  $\text{K}_4\text{C}_{60}$  from 190 K to 250 K showing a change in the  $^{13}\text{C}$  line shape.

that this quadrupole effect progressively increases when the temperature is lowered from 280 to 230 K.

Where does this EFG come from? As represented in Fig. 9, in the sc phase, the environment of  $^{23}\text{Na}$  is quite asymmetric. This could favor a displacement of Na along the cube diagonal (indicated by the arrow) towards the hexagonal ring, as was observed by x ray in the structurally similar  $\text{Na}_2\text{CsC}_{60}$ ,<sup>36</sup> that would create an electric-field gradient.  $\text{C}_{60}$  molecular motions have to be reduced to allow this displacement. More precisely, rotation around one axis could still exist (and it probably persists down to about 180 K where we observe the peak in  $^{13}\text{C}$  NMR  $1/T_1$ ), but reorientation of the rotation axis must be nearly prohibited [such a decomposition of the molecular motion was proposed for  $\text{K}_3\text{C}_{60}$  (Ref. 28)]. Here, we believe that this “slow” reorientational motion is slowing down progressively when we begin to observe static quadrupole effects around 280 K and is totally frozen below 250 K.

It is quite striking that the  $^{23}\text{Na}$  shift, plotted again in Fig. 9 for comparison, starts to increase just as the EFG disappears and this strongly suggests a relation between the two effects. One possibility is that this increase reflects that of the hyperfine coupling as the Na atom moves because of the distortion. However, we have seen in the preceding section that the shift can be rather well understood in terms of a singlet-triplet susceptibility, so that we believe that it is the susceptibility that starts to increase suddenly when the distortion disappears. This indeed would explain the steeper increase of the shift compared to the singlet-triplet model noted in Fig. 8. This suggests that the distortion stabilizes the singlet state and that triplet states can only be significantly populated when it disappears. The exact microscopic origin of such an interplay is not yet clear. The orbital moment of the triplet distortion might be incompatible with the crystal field induced by the structural distortion, which forbids their existence.

### C. Change of the symmetry of the $\text{C}_{60}$ molecular motion in $\text{K}_4\text{C}_{60}$

In  $\text{K}_4\text{C}_{60}$ , there is no ordering transition but we report here in Fig. 10 modifications of the  $^{13}\text{C}$  line shape that indi-

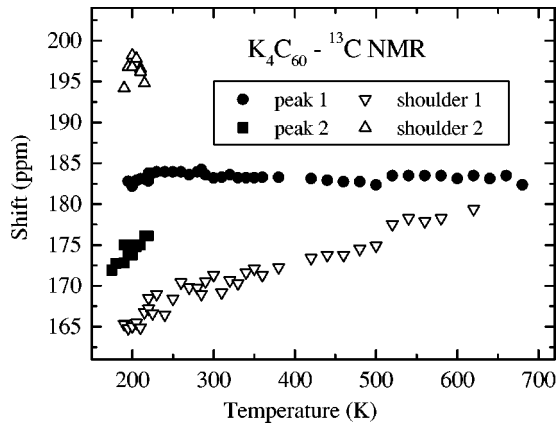


FIG. 11. Shifts of the different peaks indicated on Fig. 10 in the  $^{13}\text{C}$  NMR spectrum of  $\text{K}_4\text{C}_{60}$  from 200 to 700 K.

cate a structural evolution. At high temperatures, the  $^{13}\text{C}$  spectrum consists of one narrow symmetric line, as expected because of the motional narrowing of the spectrum. However, a shoulder appears below 580 K on the low-frequency side, and becomes progressively better defined as the temperature is lowered. This line shape is characteristic of a small axial anisotropy and probably corresponds to the development of the uniaxial motion, which would not be completely averaged anymore by molecular reorientations. Note that this anisotropy is however still very small with respect to the low-temperature one (200 ppm). Below 250 K, the spectral weight is quite suddenly transferred to the right of the spectra, as noted in the figure by the appearance of peak 2 and shoulder 2. Figure 11 summarizes the situation by displaying the shift of the various peaks as a function of temperature. This complex behavior is not understood, but it is probably related to a change in the symmetry of the molecular motion. This shows that, even though there is no reported structural transition in  $\text{K}_4\text{C}_{60}$  in this temperature range, the local symmetry changes. Let us recall that a true structural transition has been detected by differential thermal analysis in  $\text{K}_3\text{C}_{60}$  at 200 K that has never been associated so far to a precise structural distortion.<sup>28</sup>

As a matter of fact,  $1/T_1$  saturates precisely around 250 K, as can be checked in Fig. 5. This coincidence bears some similarity with the case of  $\text{Na}_2\text{C}_{60}$ , which incites us to take it seriously. When discussing the  $1/T_1 = cst$  regime, we mentioned that it could be understood by a coupling to a fixed number of triplet states. This would require that the structural change at 250 K favors the triplet states almost exclusively.

Very recently an infrared study of  $\text{K}_4\text{C}_{60}$  has revealed a splitting of the two high-frequency  $T_{1u}$  modes from a doublet above 250 K to a triplet at lower temperature.<sup>38</sup> This observation definitely establishes a symmetry breaking in this temperature range, although the exact nature of the JTD and their ordering in the high- and low-temperature phases is still unclear.

#### IV. COEXISTENCE WITH A METALLIC CHARACTER?

So far, our study has been mainly focused on the molecular singlet-triplet excitations that dominate the high-

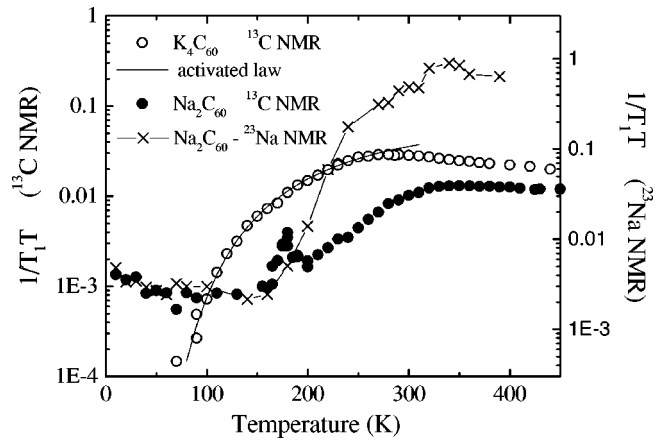


FIG. 12. Comparison of  $1/T_1T$  for  $^{13}\text{C}$  and  $^{23}\text{Na}$  in  $\text{Na}_2\text{C}_{60}$  and  $^{13}\text{C}$  in  $\text{K}_4\text{C}_{60}$  as a function of temperature. Note the logarithmic scale. The solid line is the activated law of Fig. 5 for  $\text{K}_4\text{C}_{60}$ .

temperature behavior. However, we have seen that a Pauli-like contribution seems to be present in  $\chi$  for  $\text{Na}_2\text{C}_{60}$ , which could imply that  $\text{Na}_2\text{C}_{60}$  is weakly metallic. Such a possible coexistence of bandlike excitations with typically molecular ones is an important issue. We therefore pay, hereafter, particular attention to this subject by studying the low-temperature behavior of  $1/T_1$ , which probes the nature of the excitations of the ground state of this system.

The temperature dependence of  $1/T_1T$  at low  $T$  in  $\text{Na}_2\text{C}_{60}$  and  $\text{K}_4\text{C}_{60}$  is emphasized in the logarithmic plot of Fig. 12. It can be seen that in  $\text{Na}_2\text{C}_{60}$ ,  $1/T_1$  deviates from the activated behavior below 100 K; actually  $1/T_1T$  tends to a constant value for  $^{13}\text{C}$  and  $^{23}\text{Na}$ . On the other hand, in  $\text{K}_4\text{C}_{60}$ ,  $1/T_1T$  follows the activated law of Fig. 5 down to the lowest measured temperature. The very long value for  $T_1$  in this system at this temperature prevents us from studying this behavior further. In  $\text{Rb}_4\text{C}_{60}$ , the low-temperature data do not follow the activated behavior but were ascribed to a much smaller gap (10 meV).<sup>7</sup> As  $1/T_1T = cst$  is the Korringa law expected in a metal, this reinforces the possibility of a weak metallicity of  $\text{Na}_2\text{C}_{60}$ . Before concluding firmly on this eventuality, we have to consider possible complications in the interpretation of the relaxation data.

#### A. Relaxation curves

To be sure of the temperature dependence of  $1/T_1$  down to the lowest temperature, one has to check first that the shape of the nuclear magnetization recovery curve after saturation is not changing. This question is not trivial in fullerenes as a nonexponentiality always appears at low temperatures, giving some ambiguity in the actual definition of an average  $T_1$  value. In  $\text{Na}_2\text{C}_{60}$  and  $\text{K}_4\text{C}_{60}$ , this happens below 150 K, but Fig. 13 shows that the relaxation curves can be *scaled together* for different temperatures. This means that they keep a similar shape with varying temperature within experimental accuracy, and therefore a single time parameter can be used to characterize the variation of the relaxation below 150 K. This allows to define a  $T_1$  value which depends



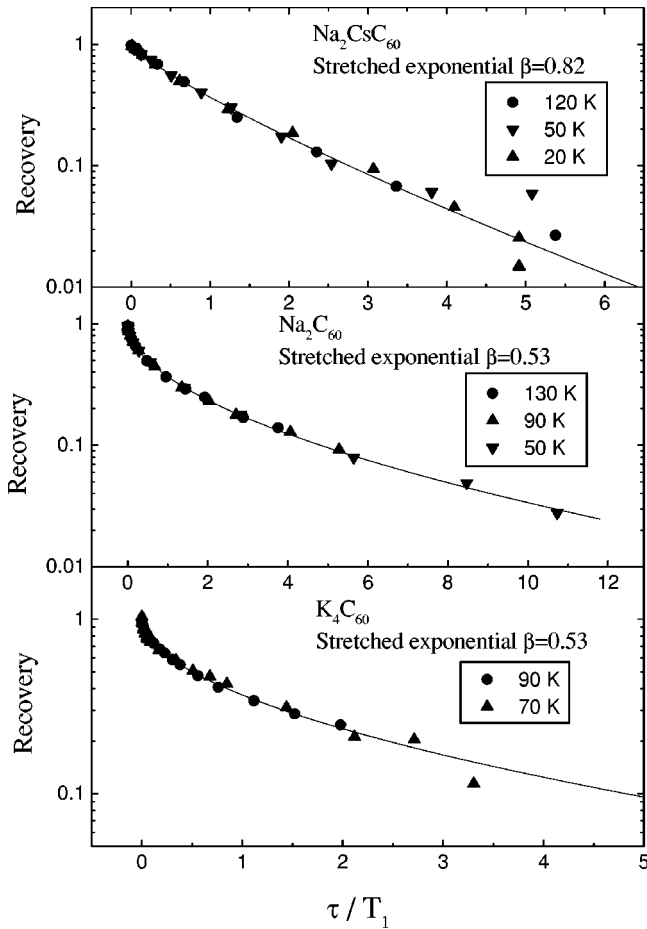


FIG. 13. Recovery curves for  $^{13}\text{C}$  in  $\text{Na}_2\text{CsC}_{60}$ ,  $\text{Na}_2\text{C}_{60}$ , and  $\text{K}_4\text{C}_{60}$ , for different temperatures (see legend).  $[M(\tau) - M_0]/M_0$  is plotted on a logarithmic scale, where  $M(\tau)$  is the echo intensity at a delay  $\tau$  after the saturation pulse and  $M_0$  is the intensity at saturation ( $\tau \rightarrow \infty$ ). The recovery curves are scaled for the different temperatures by normalizing  $\tau$  with the value of  $T_1$  extracted from a stretched exponential fit with an exponent  $\beta$  indicated on the graph. The solid line is a fit to such a recovery law.

somewhat on the expression used to fit the magnetization recovery curve, although its temperature dependence does not.

In  $\text{Na}_2\text{C}_{60}$ , the relaxation curves can be described by a stretched exponential  $M(t) = \exp[-(t/T_1)^\beta]$  with values of  $\beta$  ranging from 0.5 to 0.6. Within experimental accuracy, many different laws could describe this dependence, from multiexponential recovery (two sites or more) to stretched exponential. We choose the latter not for physical reasons but because it allows to compare easily the relaxation in different systems. The same fit applies in  $\text{K}_4\text{C}_{60}$ , although the experimental accuracy is not sufficient to determine  $\beta$  very precisely. All the curves presented in Fig. 13 are fitted with  $\beta=0.53$  to illustrate the adequacy of this fitting function. For comparison, the recovery curves in  $\text{Na}_2\text{CsC}_{60}$  are also plotted, they are typical of recovery curves found in  $A_3\text{C}_{60}$  compounds.<sup>25,39,40</sup> Here, the deviation from exponentiality is smaller, as illustrated by the value of the exponent for the stretched exponential ( $\beta=0.82$ ) closer to unity.

It is widely believed that, for  $A_3\text{C}_{60}$ , the nonexponentiality stems from a differentiation between three slightly inequivalent  $^{13}\text{C}$  sites on one  $\text{C}_{60}$  ball.<sup>39,40</sup> When the motion of the balls is frozen, the inhomogeneous local charge distribution between these sites leads to a distribution of  $T_1$  resulting in a nonexponential recovery. The difference found for the exponent  $\beta$  between  $A_3\text{C}_{60}$  and the compounds studied here is significant enough to wonder whether the same explanation could be applied to them. As the structure is much more different between  $\text{Na}_2\text{C}_{60}$  and  $\text{K}_4\text{C}_{60}$  than  $\text{Na}_2\text{C}_{60}$  and  $\text{Na}_2\text{CsC}_{60}$ , it seems unlikely that the change of relaxation behavior has a structural origin. It could *a priori* be due to the addition of an extrinsic term caused by paramagnetic impurities, but the analysis presented in the following section makes such a contribution unlikely. We then suggest that it is indeed related to a different nature of the relaxation in  $\text{K}_4\text{C}_{60}$  and  $\text{Na}_2\text{C}_{60}$ , due to the fact that electrons are more localized on the ball.

### B. Role of impurities in the low- $T$ relaxation

In insulating solids, as the intrinsic  $T_1$  becomes long at low temperature, even a small number of paramagnetic impurities could become a dominant relaxation process. As a matter of fact, a rather high concentration of paramagnetic impurities seems to always be present in these compounds and their role in the low- $T$  relaxation must be considered. Paramagnetic impurities would likely produce a saturation of  $1/T_1$  at low temperatures, i.e., an increase of  $1/T_1 T$ .<sup>31</sup> One could imagine that this “compensates” the decrease of the singlet-triplet component to mimic a  $1/T_1 T = cst$  law.

The comparison between  $\text{Na}_2\text{C}_{60}$  and  $\text{K}_4\text{C}_{60}$  can help to test whether this is likely. The paramagnetic contribution should have the same characteristics in both compounds but be proportional to the number of paramagnetic impurities in a given sample. We have characterized the paramagnetic impurity content by ESR on samples issued from the same batches as the NMR ones. From the low-temperature Curie tail observed by ESR, the impurity concentrations are estimated to be about 2% per  $\text{C}_{60}$  in  $\text{Na}_2\text{C}_{60}$  and 1% in  $\text{K}_4\text{C}_{60}$ . We do observe longer  $T_1$  in  $\text{K}_4\text{C}_{60}$ , but they are too long (by already a factor 10 at 70 K, as can be seen on Fig. 12) to be explained by a difference of a factor 2 in impurity content. Data in  $\text{K}_4\text{C}_{60}$  allow to set a maximal value for the contribution of impurities in  $\text{Na}_2\text{C}_{60}$  to  $1/T_1 T < 3 \times 10^{-4} \text{ (sec K)}^{-1}$  at 70 K, which is too small to be responsible for the deviation from the activated law.

Another independent indication of the intrinsic character of the relaxation comes from the comparison with  $^{23}\text{Na}$  NMR. We have seen in Sec. III C that only the central transition is observed for this nucleus, which automatically results in a nonexponential relaxation.<sup>31</sup> It is then delicate to base a discussion on the *shape* of the relaxation curves. Nevertheless, Fig. 12 shows a very similar temperature dependence for the two nuclei. As the increase of  $1/T_1$  between 150 K and 300 K has very different magnitudes for  $^{13}\text{C}$  and  $^{23}\text{Na}$  (probably because a quadrupole term is present in  $^{23}\text{Na}$   $1/T_1$ ), it seems impossible that an intrinsic and extrinsic term

could compensate at low  $T$  to give an identical temperature dependence on the two nuclei over a temperature range as large as 150 K.

We then conclude that our experiment probes a metallic character in  $\text{Na}_2\text{C}_{60}$ . As a proof of consistency, the value of  $n(E_f)$  needed to explain the  $1/T_1 T = cst$  law by the Korringa mechanism can be estimated to be  $1 \text{ eV}^{-1}$ , which agrees with the value of  $\chi \approx 7 \times 10^{-5} \text{ emu/mol}$  found by  $^{23}\text{Na}$  NMR.<sup>11</sup>

## V. CONCLUSION

In conclusion, the main properties of  $\text{Na}_2\text{C}_{60}$  and  $\text{K}_4\text{C}_{60}$  appear similar and therefore represent the typical behavior of two electrons or two holes in the  $t_{1u}$  band. Molecular excitations dominate their properties; starting from a singlet ground state, excitations to a triplet one are thermally accessible. We attribute the existence of these two states to the two most stable Jahn-Teller distortions, which have, respectively, a singlet and triplet ground state. We further show that this molecular approach is insufficient to describe the full temperature range.  $\chi$  and  $1/T_1$  seem to change more suddenly than one would expect in a completely thermal process. The structural transition from fcc to sc is not found essential in the variation of the properties of  $\text{Na}_2\text{C}_{60}$ . However, in both compounds, we evidence changes in the structure concomitant with the change in  $1/T_1$ , probably associated with the slowing down of molecular motions. This suggests that there is a coupling between the structure and the stabilization of JTD, maybe due to crystal-field effects acting on the orbital moment of the different Jahn-Teller configurations.

We also give evidence that the singlet states are not strictly localized at one molecule. This is most clear by the low-energy excitations observed in  $\text{Na}_2\text{C}_{60}$  at low temperatures, which are best described by a metallic-like process with a small value of the density of states. Interactions between the balls also renormalize the value of the ST gap and yield to deviations with respect to a purely molecular model in the behavior of  $1/T_1$  and  $\chi$ .

The interplay between molecular and bandlike properties is certainly one of the most intriguing feature of fullerides

and a good understanding of this effect is a prerequisite before addressing the case of  $\text{A}_3\text{C}_{60}$ . Two different kind of metal-insulator transitions clearly take place in fullerides, one in  $\text{Rb}_4\text{C}_{60}$  as a function of lattice spacing, which has been observed under applied pressure,<sup>7</sup> and one as a function of doping if one could go continuously from  $\text{Na}_2\text{C}_{60}$  to  $\text{A}_3\text{C}_{60}$  to  $\text{A}_4\text{C}_{60}$ . The fact that these superconducting fullerides are surrounded by almost insulating phases has not always received much attention, probably because it is not easily possible to go from one phase to the other. When transport is measured as a function of alkali doping, usually on thin films,<sup>41</sup> no sharp metal to insulator transitions can be observed, which gives the impression that a rigid band filling picture could be applied. However, it is known that phase separation could occur in these films. The well-established fact that superconductivity is restricted to a very limited doping range around  $n=3$  is a strong deviation from the expectations of the BCS theory usually applied to these materials. This indicates particular properties for the *integer filling*  $n=3$ . This might also be true for  $n=2$  and 4, and the metallic state could be nearly suppressed *only* in these two cases. This importance of integer fillings might be related to the stronger correlation effects that appear in this case combined with the possibility of stabilizing molecular JTD. On one hand, the case of  $\text{Na}_2\text{C}_{60}$  studied here or that of  $\text{Rb}_4\text{C}_{60}$  under applied pressure indicate that metallic and molecular properties are not exclusive but *do* coexist. On the other hand, the study of  $\text{CsC}_{60}$  that we will present in paper II shows that JTD's  $\text{C}_{60}^{2-}$  are particularly stable, even when there is nominally one electron per  $\text{C}_{60}$ . We will develop in paper III the idea that the remarkable properties of  $\text{A}_3\text{C}_{60}$  are due to an optimum cooperation between metallic and molecular aspects, because of its symmetric position between  $n=2$  and 4.

## ACKNOWLEDGMENTS

We thank E. Tosatti, N. Manini, and K. Kamaras for useful discussions. Financial support from the TMR program of the European Commission is acknowledged (Research network "FULPROP" ERBMRMXVT970155).

<sup>1</sup>S.C. Erwin, in *Buckminsterfullerenes*, edited by W.E. Billups and M.A. Ciufolini (VCH, New York, 1992).

<sup>2</sup>R.F. Kiefl *et al.*, Phys. Rev. Lett. **69**, 2005 (1992).

<sup>3</sup>P. Petit, *et al.*, *Progress in Fullerene Research* edited by H. Kuzmany, J. Fink, M. Mehring, and S. Roth (World Scientific, Singapore, 1994), p. 148.

<sup>4</sup>I. Lukyanchuk, N. Kirova, F. Rachdi, C. Goze, P. Molinie, and M. Mehring, Phys. Rev. B **51**, 3978 (1995).

<sup>5</sup>G. Zimmer, M. Helme, M. Mehring, and F. Rachdi, Europhys. Lett. **27**, 543 (1994).

<sup>6</sup>G. Zimmer, M. Mehring, C. Goze, and F. Rachdi, Phys. Rev. B **52**, 13 300 (1995).

<sup>7</sup>R. Kerkoud, P. Auban-Senzier, D. Jerome, S. Brazovskii, I. Luk'yanchuk, N. Kirova, F. Rachdi, and C. Goze, J. Phys.

Chem. Solids **57**, 143 (1996).

<sup>8</sup>R. Hesper, L.H. Tjeng, A. Heeres, and G.A. Sawatzky, Phys. Rev. B **62**, 16 046 (2000), and references therein.

<sup>9</sup>Y. Iwasa and T. Kaneyasu, Phys. Rev. B **51**, 3678 (1995).

<sup>10</sup>M. Knupfer and J. Fink, Phys. Rev. Lett. **79**, 2714 (1997).

<sup>11</sup>V. Brouet, H. Alloul, L. Thien-Nga, S. Garaj, and L. Forró, Phys. Rev. Lett. **86**, 4680 (2001).

<sup>12</sup>O. Zhou and D. Cox, J. Phys. Chem. Solids **53**, 1373 (1992).

<sup>13</sup>C.A. Kuntscher, G.M. Bendele, and P.W. Stephens, Phys. Rev. B **55**, R3366 (1997).

<sup>14</sup>G. Oszlanyi, G. Baumgartner, G. Faigel, L. Granasy, and L. Forró, Phys. Rev. B **58**, 5 (1998).

<sup>15</sup>O. Gunnarsson, S. C Erwin, E. Koch, and R.M. Martin, Phys. Rev. B **57**, 2159 (1998); J.E. Han, E. Koch, and O. Gunnarsson,

- Phys. Rev. Lett. **84**, 1276 (2000).
- <sup>16</sup>T. Yildirim, J.E. Fischer, A.B. Harris, P.W. Stephens, D. Liu, L. Brard, R.M. Strongin, and A.B. Smith, Phys. Rev. Lett. **71**, 1383 (1993).
- <sup>17</sup>N. Manini, E. Tosatti, and A. Auerbach, Phys. Rev. B **49**, 13 008 (1994).
- <sup>18</sup>M. Fabrizio and E. Tosatti, Phys. Rev. B **55**, 13 465 (1997).
- <sup>19</sup>M. Capone, M. Fabrizio, P. Giannozzi, and E. Tosatti, Phys. Rev. B **62**, 7619 (2000).
- <sup>20</sup>V. Brouet, H. Alloul, and L. Forró following paper, Phys. Rev. B **66**, 155123 (2002).
- <sup>21</sup>V. Brouet, H. Alloul, S. Garaj, and L. Forró, this issue, Phys. Rev. B **66**, 155124 (2002).
- <sup>22</sup>C.H. Pennington and V.A. Stenger, Rev. Mod. Phys. **68**, 855 (1996).
- <sup>23</sup>R. Tycko, G. Dabbagh, R.M. Fleming, R.C. Haddon, A.V. Makhija, and S.M. Zahurak, Phys. Rev. Lett. **67**, 1886 (1991).
- <sup>24</sup>J. Reichenbach, F. Rachdi, I. Luk'yanchuk, M. Ribet, G. Zimmer, and M. Mehring, J. Chem. Phys. **101**, 4585 (1994).
- <sup>25</sup>M. Mehring, F. Rachdi, and G. Zimmer, Philos. Mag. B **70**, 787 (1994).
- <sup>26</sup>R. Tycko, G. Dabbagh, M.J. Rosseinsky, D.W. Murphy, A.P. Ramirez, and R.M. Fleming, Phys. Rev. Lett. **68**, 1912 (1992).
- <sup>27</sup>C.P. Slichter, *Principles of Magnetic Resonance* (Springer-Verlag, Berlin, 1989).
- <sup>28</sup>Y. Yoshinari, H. Alloul, G. Kriza, and K. Holczer, Phys. Rev. Lett. **71**, 2413 (1993).
- <sup>29</sup>N. Bloembergen, E.M. Purcell, and R.V. Pound, Phys. Rev. **73**, 679 (1948).
- <sup>30</sup>Y. Yoshinari, H. Alloul, V. Brouet, G. Kriza, K. Holczer, and L. Forró, Phys. Rev. B **54**, 6155 (1996).
- <sup>31</sup>A. Abragam, *Principle Of Nuclear Magnetism* (Oxford University Press, Oxford, 1961).
- <sup>32</sup>R.D. Johnson, C.S. Yannoni, H.C. Dorn, J.R. Salem, and D.S. Bethune, Science **255**, 1235 (1992).
- <sup>33</sup>A. Penicaud *et al.* (unpublished).
- <sup>34</sup>P. Launois, R. Moret, N.R. de Souza, J.A. Azamar-Barrios, and A. Pénicaud, Eur. Phys. J. B **15**, 445 (2000).
- <sup>35</sup>T. Yildirim, J.E. Fischer, R. Dinnebier, P.W. Stephens, and C.L. Lin, Solid State Commun. **93**, 26 (1995).
- <sup>36</sup>K. Prassides, C. Christides, I.M. Thomas, J. Mizuki, K. Tanigaki, I. Hirose, and T.W. Ebbesen, Science **263**, 950 (1994).
- <sup>37</sup>V. Brouet, H. Alloul, T. Saito, and L. Forro, in *Electronic Properties of Novel Materials—Molecular Nanostructures*, edited by H. Kuzmany, J. Fink, M. Mehring, and S. Roth, AIP Conf. Proc. No. 544 (AIP, New York, 2000), p. 24.
- <sup>38</sup>K. Kamaras, G. Klupp, D.B. Tanner, A.F. Hebard, N.M. Nemes, and J.E. Fischer, Phys. Rev. B **65**, 052103 (2002).
- <sup>39</sup>K. Holczer, O. Klein, H. Alloul, Y. Yoshinari, F. Hippert, S.-M. Huang, R.B. Kaner, and R.L. Whetten, Europhys. Lett. **23**, 63 (1993).
- <sup>40</sup>Y. Maniwa *et al.*, J. Phys. Soc. Jpn. **63**, 1139 (1994).
- <sup>41</sup>F. Stepniak, P.J. Benning, D.M. Poirier, and J.H. Weaver, Phys. Rev. B **48**, 1899 (1993).